Recombinant high-mobility group box 1 induces cardiomyocyte hypertrophy by regulating the 14-3-3η, PI3K and nuclear factor of activated T cells signaling pathways

FEIFEI SU[1,2*], MIAOQIAN SHI[3*], JIAN ZHANG[4*], YAN LI[2] and JIANWEI TIAN[1]

[1]Department of Cardiology, Air Force Medical Center, People's Liberation Army, Beijing 100142;
[2]Department of Cardiology, Tangdu Hospital Affiliated to The Fourth Military Medical University, Xi'an, Shaanxi 710038;
[3]Department of Cardiology, The Seventh Medical Centre of The People's Liberation Army General Hospital, Beijing 100700;
[4]Department of Cardiology, Beijing Chest Hospital Heart Center, Capital Medical University, Beijing 101149, P.R. China

Abstract. High-mobility group box 1 (HMGB1) is released by necrotic cells and serves an important role in cardiovascular pathology. However, the effects of HMGB1 in cardiomyocyte hypertrophy remain unclear. Therefore, the aim of the present study was to investigate the potential role of HMGB1 in cardiomyocyte hypertrophy and the underlying mechanisms of its action. Neonatal mouse cardiomyocytes (NMCs) were co-cultured with recombinant HMGB1 (rHMGB1). Wortmannin was used to inhibit PI3K activity in cardiomyocytes. Subsequently, atrial natriuretic peptide (ANP), 14-3-3 and phosphorylated-Akt (p-Akt) protein levels were detected using western blot analysis. In addition, nuclear factor of activated T cells 3 (NFAT3) protein levels were measured by western blot analysis and observed in NMCs under a confocal microscope. The results revealed that rHMGB1 increased ANP and p-Akt, and decreased 14-3-3η protein levels. Furthermore, wortmannin abrogated the effects of rHMGB1 on ANP, 14-3-3η and p-Akt protein levels. In addition, rHMGB1 induced nuclear translocation of NFAT3, which was also inhibited by wortmannin pretreatment. The results of this study suggest that rHMGB1 induces cardiac hypertrophy by regulating the 14-3-3η/PI3K/Akt/NFAT3 signaling pathway.

Introduction

High-mobility group box 1 (HMGB1) is released by activated cells, including cardiomyocytes and damaged or necrotic

---

Correspondence to: Dr Feifei Su, Department of Cardiology, Air Force Medical Center, People's Liberation Army, 30 Fucheng Road, Haidian, Beijing 100142, P.R. China
E-mail: shijian@fmmu.edu.cn

*Contributed equally

cells, and serves as an inflammatory cytokine. In addition, HMGB1 serves an important role in multiple organ pathologies, including cerebral, liver, lung and renal injury, and rheumatoid arthritis (1). It is likely that the specific properties of HMGB1 exhibit an effect on cardiomyocytes. Recently, it has been suggested that HMGB1 is involved in cardiovascular diseases (2), such as cardiac fibrosis, myocardial ischemia-reperfusion injury, heart transplantation, aortic valve calcification and sepsis-associated myocardial dysfunction (3-7). Although these previous reports have revealed that HMGB1 serves an essential role in the cardiovascular system, in which our previous study (8) also reported that HMGB1 induced cardiomyocyte hypertrophy, its physiological function in cardiomyocytes requires further investigation.

Cardiac hypertrophy is induced by several factors, including inflammatory factors and stresses, such as hypoxia (9). This process is initially considered beneficial, but it may progress to heart failure (10,11) under prolonged stress (12). It has been suggested that cardiac hypertrophy may be attenuated by controlling inflammation (13). HMGB1 acts as an inflammatory cytokine and serves an important role in cardiovascular pathology (14). Therefore, increased levels of circulating HMGB1 may be associated with human heart disease (15). For example, exogenous HMGB1 treatment in acute myocardial infarction induces cardiomyocyte survival by attenuating apoptosis and AMP-activated protein kinase-dependent autophagy (16). Our previous study demonstrated that HMGB1 may induce cardiomyocyte hypertrophy (8). In addition, HMGB1 may be partially derived from cardiac myocytes under pressure overload and may serve a crucial role in cardiac dysfunction (17). Notably, maintenance of stable nuclear HMGB1 levels prevents heart hypertrophy and failure by inhibiting DNA damage (18). However, to the best of our knowledge, the direct effects of exogenous HMGB1 treatment on cardiomyocytes remain elusive.

14-3-3 proteins are distributed ubiquitously in all eukaryotic organisms and serve a major role in stress response in several cells, including cardiomyocytes. The 14-3-3 protein family includes several highly conserved acid proteins, named according to their different isoforms (19). The 14-3-3 protein

family includes several highly conserved acid proteins, named according to their different isoforms (β, ε, η, γ, τ, σ and ζ) detected in the cell cytoplasm and nucleus (20,21). 14-3-3η has been reported to serve an essential role in myocardial metabolism (22,23). Additionally, depletion of 14-3-3η increases cardiac hypertrophy, inflammation, fibrosis and apoptosis (24). It has previously been suggested that 14-3-3 proteins regulate the nuclear translocation of the nuclear factor of activated T cells (NFAT) (25,26), which in turn may induce pathological cardiac hypertrophy (27-29). In addition, a recent study has revealed that simvastatin upregulates 14-3-3 expression, which ultimately exerts beneficial effects through cardioprotection against pressure overload (30). In addition, 14-3-3 proteins interact with PI3K and NFAT3-mediated transcription in cardiomyocytes (19), which in turn phosphorylates its downstream target, Akt, resulting in physiological cardiac growth (31,32). The aforementioned results indicate that 14-3-3 proteins may be involved in the process of cardiac hypertrophy. However, whether HMGB1 interacts with 14-3-3 proteins to affect cardiac hypertrophy remains unclear, and, to the best of our knowledge, there are no studies on the association between HMGB1 and 14-3-3 proteins in cardiac hypertrophy.

Therefore, the present study hypothesized that HMGB1 may induce cardiomyocyte hypertrophy by regulating the 14-3-3 and PI3K/Akt signaling pathways. To test this hypothesis, neonatal mouse cardiomyocytes (NMCs) were isolated and treated with HMGB1. Subsequently, NMCs were treated with wortmannin, a specific PI3K inhibitor. Furthermore, to assess the nuclear translocation of NFAT in NMCs, the effects were observed by confocal microscopy.

Materials and methods

Preparation of NMCs and treatment. NMCs were isolated from 100 C57BL/6 mice (male; weight, 2±0.5 g; age, 1-3 days old), which were housed in a pathogen free facility with 50% humidity at 22˚C, with a 12-h light/dark cycle and free access to food and water. Mice were obtained from the Animal Center of the Fourth Military Medical University (Xi'an China)]. The mice were sacrificed by decapitation and heart cell isolation was performed using the Pierce Primary Cardiomyocyte Isolation kit (Thermo Fisher Scientific, Inc.), according to the manufacturer's protocol. A monolayer of isolated NMCs was plated at a density of $3x10^6$ cells/plate. NMCs were cultured in DMEM (Gibco; Thermo Fisher Scientific, Inc.) containing 1% penicillin-streptomycin (Thermo Fisher Scientific, Inc.) and 10% FBS (Thomas Scientific, Inc.) at 37˚C in a humidified atmosphere with 5% CO_2. The presence of fibroblasts was minimized by the addition of cardiomyocyte growth supplement (dilution, 1:1,000; Thermo Fisher Scientific, Inc.). Subsequently, NMCs were divided into the following four groups: The control (Ctrl) group; the wortmannin (Wort; kindly provided by Dr Jun L)-treated group; the recombinant HMGB1-treated (rHMGB1) group; and the rHMGB1 plus Wort (rHMGB1+Wort) group. In addition, rHMGB1 and wortmannin treatment of NMCs was performed according to our previous study (8). NMCs were treated with 200 ng/ml rHMGB1 (Sigma-Aldrich; Merck KGaA) or PBS for 24 h in the rHMGB1 or Ctrl groups, respectively, and with 100 nmol/l

wortmannin for 60 min prior to exposure to PBS or rHMGB1 in the Wort or rHMGB1+Wort groups, respectively.

NMC protein synthesis measurement. Following treatment, NMCs were trypsinized, counted using a cell counting chamber (Beckman Coulter, Inc.) and lysed for further protein detection. Subsequently, protein concentration was determined using a Bradford protein assay (Bio-Rad Laboratories, Inc.). Finally, the protein synthesis per cell was calculated by dividing the total amount of protein by the number of NMCs.

Reverse transcription-quantitative PCR (RT-qPCR). Total RNA was extracted from NMCs using the TRIzol® reagent (Invitrogen; Thermo Fisher Scientific, Inc.). RNA samples were quantified spectrophotometrically at 260 nm. Subsequently, RT-qPCR was performed as previously described (8). Briefly, RNA was exposed to RNAse-free DNase I and 5 μg total RNA was reverse transcribed into cDNA using oligo(dT) and M-MuLV reverse transcriptase (Promega Corporation). The reverse transcription products served as templates for PCR using gene-specific primers (Table I) (33). qPCR was subsequently performed using a TaqMan™ Fast Advanced Master Mix (Applied Biosystems; Thermo Fisher Scientific, Inc.) using the 7500 Sequence Detector Real-Time PCR system (Applied Biosystems; Thermo Fisher Scientific, Inc.). The thermocycling conditions were as follows: Initial step at 95˚C for 10 min, followed by 40 cycles at 95˚C for 15 sec and 60˚C for 1 min. Fluorescence signals of each gene were recorded during the elongation phase of each PCR cycle. The melting curve analysis was used to confirm the amplification specificity, and the RNA abundance was expressed as ΔΔCq. GAPDH expression served as the internal control, and each gene was quantified in duplicate. Finally, the RT-qPCR data were analyzed using the $2^{-\Delta\Delta Cq}$ method (34).

Western blot analysis. NMCs were rinsed with PBS and lysed in buffer [Cell Lysis buffer (10X); cat. no. 9803; Cell Signaling Technology, Inc.] on ice. Subsequently, cell lysates were centrifuged (2,000 x g; 5-7 min; 4˚C), and the supernatant was collected. Following a Bradford assay to determine protein concentration, equal amounts of proteins (20 μg) were diluted in sample buffer (Thermo Fisher Scientific, Inc.), boiled and separated using 15% SDS-PAGE (Thermo Fisher Scientific, Inc.). The separated proteins were transferred to a nitrocellulose membrane (LI-COR Biosciences). Following blocking in 5 ml 1X Odyssey® blocking buffer (LI-COR Biosciences) for 1 h at room temperature, the nitrocellulose membranes were incubated with primary antibodies at 4˚C for 12 h. Subsequently, membranes were washed with 1X PBS-T (PBS with 0.1% Tween-20) and incubated with secondary antibodies for 1 h at room temperature. Finally, immunoreactive protein bands were analyzed by densitometry using the Odyssey® infrared imaging system (version 2.1; LI-COR Biosciences), and the specific protein bands were visualized using an Odyssey® scanner, then analyzed using Image Studio Lite version 5.0 (LI-COR Biosciences). The primary antibodies used in the present study were all diluted 1:1,000 and were: Anti-atrial natriuretic peptide (ANP; cat. no. ab126149; Abcam), anti-pan14-3-3

Table I. Primers used for reverse transcription-quantitative PCR.

Gene	Forward primer (5'→3')	Reverse primer (5'→3')
ANP	AGGCAGTCGATTCTGCTT	CGTGATAGATGAAGGCAGGAAG
BNP	TAGCCAGTCTCCAGAGCAATTC	TTGGTCCTTCAAGAGCTGTCTC
GAPDH	CCTTCCGTGTTCCTACCCC	GCCCAAGATGCCCTTCAGT

ANP, atrial natriuretic peptide; BNP, brain natriuretic peptide.

(cat. no. ab32377; Abcam), anti-14-3-3η (cat. no. ab206292; Abcam), anti-phospho-Akt (p-Akt) (cat. no. ab38449; Abcam), anti-histone (cat. no. ab1791; Abcam), anti-β-tubulin (cat. no. ab6160; Abcam), anti-NFAT3 (cat. no. orb315632; Biorbyt Ltd.) and anti-β-actin (cat. no. SC-8432; Santa Cruz Biotechnology, Inc.). The secondary antibodies were goat anti-mouse IRDye® (1:10,000; cat. no. 926-68070; LI-COR Biosciences), goat anti-rabbit IRDye® (1:10,000; cat. no. 926-32211; LI-COR Biosciences) and goat anti-rat IRDye® (1:10,000; cat. no. 926-32219; LI-COR Biosciences). In addition, β-tubulin and histone protein levels served as a loading control for the total protein lysate, the cytosol and nuclear extracts, respectively.

Confocal microscopy observation. NFAT3 localization in NMCs was analyzed using confocal microscopy. Briefly, NMCs were isolated and cultured on laminin pre-coated Lab-Tek chamber slides (Thermo Fisher Scientific, Inc.). Following treatment, cells ($1x10^5$ cells/well) were fixed with 4% paraformaldehyde at room temperature for 30 min, permeabilized using 0.2% Triton X-100 and washed with PBS. Subsequently, cells were incubated in 1 ml blocking reagent (SuperBlock Blocking Buffer; Thermo Scientific™; Thermo Fisher Scientific, Inc.) with primary rabbit anti-NFAT3 (1:200; cat. no. sc-8405; Santa Cruz Biotechnology, Inc.) and primary mouse anti-α-actinin antibodies (1:200; cat. no. A2543; Sigma-Aldrich; Merck KGaA) in a cold room at 4˚C for 24 h. Following extensive washing, NMCs were incubated with Alexa Fluor 594-labeled goat anti-rabbit (1:1,000; cat. no. Z25307; Invitrogen; Thermo Fisher Scientific, Inc.) and Alexa Fluor 488-labeled goat anti-mouse antibodies (1:1,000; cat. no. A20181; Invitrogen; Thermo Fisher Scientific, Inc.) at 4˚C for 30 min. Finally, cells were mounted with mounting media containing 2-(4-amidinophenyl)-1H-indole-6-carbox-amidine (DAPI, 1:1,000) (Vector Laboratories, Inc.; Maravai LifeSciences). A Carl Zeiss 710 confocal microscope (Carl Zeiss AG; magnification, x40) was used to image the NFAT3, α-actinin and DAPI staining.

Cell extract preparation. The cytosol and nuclear extracts from NMCs were prepared using an NE-PER extraction kit (Thermo Fisher Scientific, Inc.), according to the manufacturer's protocol. The specificity of the cytosol or nuclear extracts was verified by western blot analysis by detecting β-tubulin or histone protein expression, respectively.

Terminal deoxynucleotidyl transferase dUTP nick-end-labeling (TUNEL) assay. The NMC apoptosis rate was detected using a TUNEL assay kit (Roche Diagnostics), according to the manufacturer's protocol. Briefly, following treatment NMCs ($1x10^5$ cells/well) were fixed with 4% paraformaldehyde at room temperature for 30 min and permeabilized with 0.2% Triton X-100 at room temperature for 30 min. The cells were subsequently incubated with TUNEL reagent for 1 h at room temperature. Thereafter, the cells were mounted with a mounting medium containing DAPI (1:1,000; Vector Laboratories, Inc.) at room temperature for 10 min. The TUNEL-positive and the total number of nuclei were counted in five independent experiments (3 randomly selected fields of view) under a Nikon Eclipse 80 fluorescent microscope (magnification, x10; Nikon Corporation).

Statistical analysis. All data were analyzed using GraphPad Prism 5 (GraphPad Software, Inc.) and presented as the mean ± SEM for continuous variables. One-way ANOVA was used to assess differences among groups followed by Tukey's post hoc test. $P < 0.05$ was considered to indicate a statistically significant difference. The Ctrl group value was set as 1 to express the fold change.

Results

rHMGB1 induces NMC hypertrophy. Following exposure to rHMGB1 for 24 h, NMCs were harvested and their cellular protein content was analyzed. The results revealed that rHMGB1 treatment significantly increased the protein content per cell compared with that in the Ctrl group (Fig. 1A). Subsequently, the protein levels of ANP, a pathological cardiac hypertrophy marker, were detected using western blot analysis. Protein levels of ANP in the rHMGB1 group were significantly increased compared with those in the Ctrl group (Fig. 1B). In addition, the mRNA levels of ANP and brain natriuretic peptide (BNP), another pathological cardiac hypertrophy marker, were upregulated in the rHMGB1 group compared with those in the Ctrl group (Fig. 1C). Representative confocal images of NMCs are presented in Fig. 1D. Therefore, the present results suggest that rHMGB1 induces NMC hypertrophy.

rHMGB1 decreases 14-3-3η protein levels, which can be partially reversed by wortmannin. In the present study, western blot analysis was performed using anti-pan14-3-3 (an antibody against endogenous total 14-3-3 proteins) and anti-14-3-3η antibodies, to determine whether rHMGB1 could regulate their expression in NMCs. Following rHMGB1 treatment, 14-3-3η protein levels were decreased (Fig. 2A and B) and p-Akt levels were increased (Fig. 2A and F) in NMCs
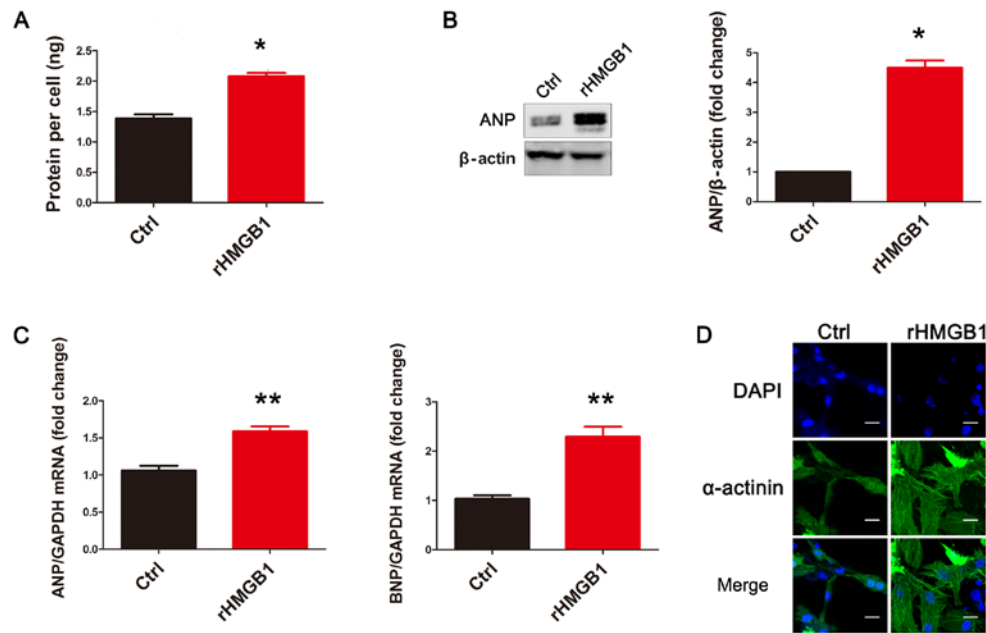
Figure 1. rHMGB1 induces NMC hypertrophy. rHMGB1 significantly increased (A) the protein content per cell, (B) ANP protein levels and (C) the mRNA levels of ANP and BNP in NMCs (n=3). Data are presented as the mean ± standard error of the mean for continuous variables. One-way ANOVA was used to assess differences among different groups. (D) Representative confocal images from the Ctrl and rHMGB1 groups (scale bar, 20 μm). Cells were stained with DAPI (blue signal) and α-actinin (green signal) to identify nuclei and cardiomyocytes, respectively. rHMGB1, recombinant high-mobility group box 1; NMC, neonatal mouse cardiomyocytes; ANP, atrial natriuretic peptide; BNP, brain natriuretic peptide; Ctrl, control; DAPI, 2-(4-amidinophenyl)-1H-indole-6-carboxamidine. *P<0.05, **P<0.01 vs. Ctrl group.
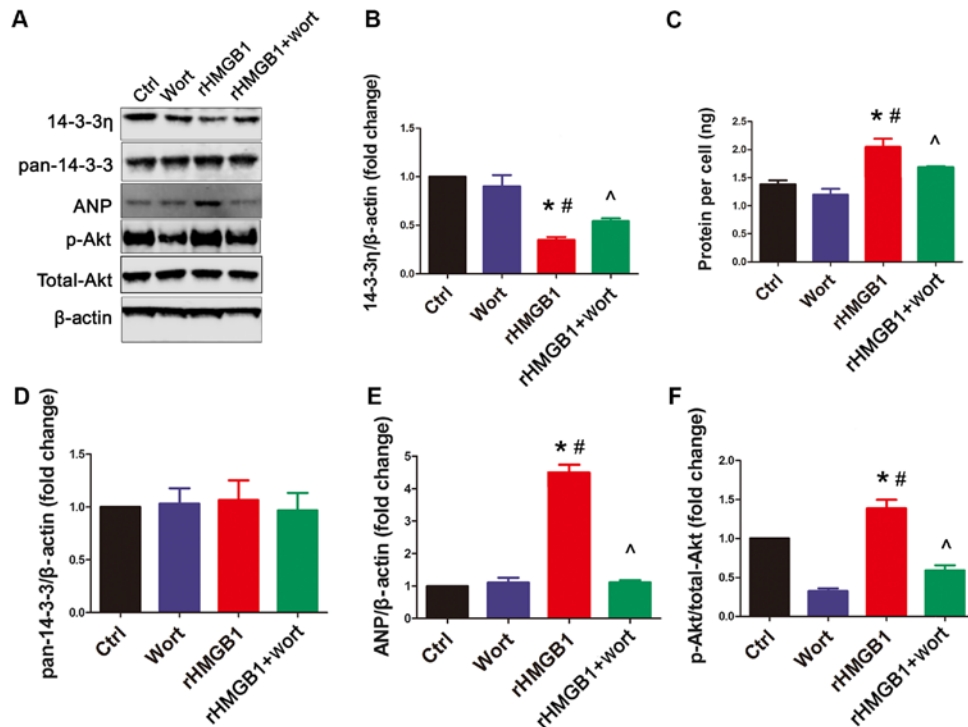

Figure 2. Effects of rHMGB1 on the protein content per cell and the protein levels of 14-3-3, ANP and p-Akt in neonatal mouse cardiomyocytes. (A) Panel represents western blot results from the different treatment groups. The other panels represent the semi-quantitative analysis of (B) 14-3-3η, (C) protein per cell, (D) pan-13-3-3, (E) ANP and (F) p-Akt/Akt from the four treatment groups. Each experiment was repeated three times (n=9). Data are presented as the mean ± SEM for continuous variables. One-way ANOVA was used to assess differences among the groups. rHMGB1, recombinant high-mobility group box 1; ANP, atrial natriuretic peptide; p-Akt, phosphorylated-Akt; Wort, wortmannin; Ctrl, control. *P<0.05 vs. Ctrl group; ^P<0.05 vs. rHMGB1 group; #P<0.05 vs. Wort group.

compared with those in the Ctrl group (Fig. 2). However, rHMGB1 treatment had no effect on the total endogenous

14-3-3 protein levels (Fig. 2A and D). Furthermore, wortmannin, a specific PI3K inhibitor, significantly inhibited the
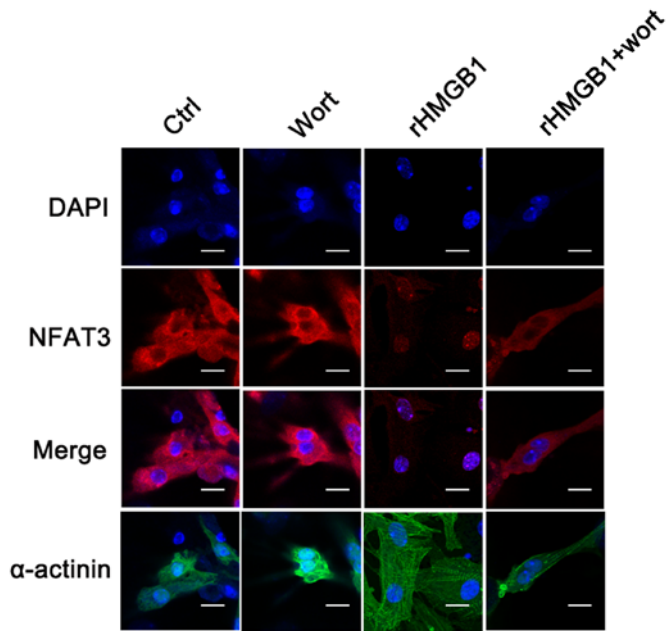
Figure 3. rHMGB1 induces NFAT3 translocation to the nucleus. Representative confocal images of NFAT3 localization in neonatal mouse cardiomyocytes in different treatment groups (scale bar, 15 μm). Red indicates NFAT3 protein, blue indicates DAPI-stained nuclei and green indicates α-actinin. Each experiment was repeated four times. rHMGB1, recombinant high-mobility group box 1; NFAT3, nuclear factor of activated T cells 3; DAPI, 2-(4-amidinophenyl)-1H-indole-6-carboxamidine; Wort, wortmannin; Ctrl, control.
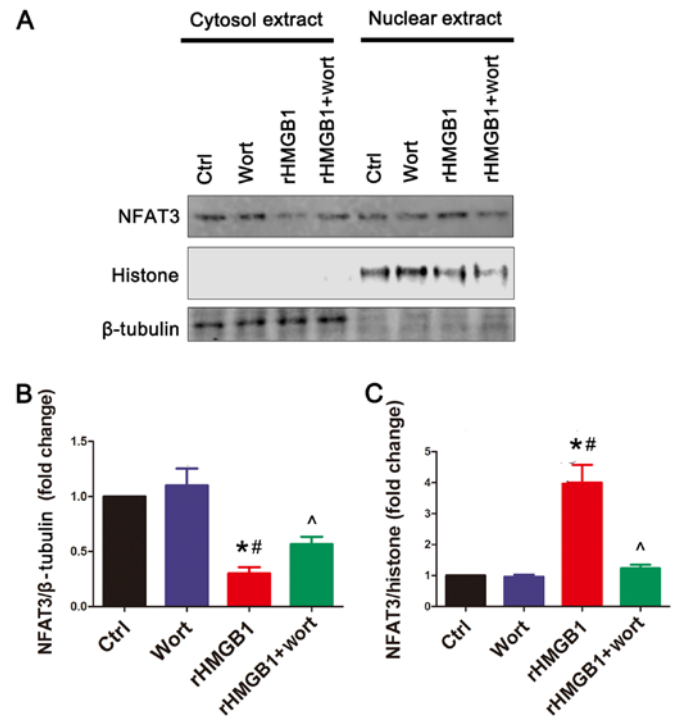

Figure 4. rHMGB1 induces NFAT3 translocation to the nucleus. (A) Representative western blot results from cytosol or nuclear extracts from different treatment groups. (B) Semi-quantitative analysis of NFAT3 in cytosol extracts, with β-tubulin serving as the loading control. (C) Semi-quantitative analysis of NFAT3 in nuclear extracts, with histone serving as a loading control. The three independent neonatal mouse cardiomyocyte cultures were used in each experiment (n=3). One-way ANOVA was used to assess differences among different groups. rHMGB1, recombinant high-mobility group box 1; NFAT3, nuclear factor of activated T cells 3; Wort, wortmannin; Ctrl, control. *P<0.05 vs. Ctrl group; $^{\wedge}$P<0.05 vs. rHMGB1 group; $^{\#}$P<0.05 vs. Wort group.

rHMGB1-mediated effects on 14-3-3η protein levels and Akt phosphorylation (Fig. 2A, B and F). However, wortmannin alone had no significant effect on 14-3-3η levels compared with the Ctrl group (Fig. 2A and B). Additionally, no changes to pan14-3-3 protein levels were observed among the different groups (Fig. 2D). Finally, the effects of rHMGB1 treatment on the protein content per cell and ANP protein levels were inhibited by wortmannin (Fig. 2A, C and E). Overall, the present results suggest that rHMGB1 regulates 14-3-3η protein levels and hypertrophy in NMCs partially through the PI3K/Akt signaling pathway.

rHMGB1 induces NFAT3 nuclear translocation, which can be inhibited by wortmannin. In the present study, confocal microscopy was used to detect the subcellular location of NFAT3 and to determine whether NFAT3 is translocated to the nucleus following rHMGB1 treatment. In the rHMGB1 group, the levels of NFAT3 in the cytosol were decreased, while those in the nuclei were increased compared with the levels of NFAT3 in the Ctrl group (Fig. 3). Notably, wortmannin pretreatment inhibited the nuclear translocation of NFAT3 following rHMGB1 treatment. The results were verified using western blot analysis, demonstrating that rHMGB1 treatment upregulated and downregulated NFAT3 protein levels in the NMC nuclear and cytoplasmic extracts, respectively (Fig. 4). Furthermore, wortmannin pretreatment reversed the effects of rHMGB1 treatment on NFAT3 protein levels (Fig. 4). The aforementioned results suggest that rHMGB1 may contribute to cardiomyocyte hypertrophy by regulating NFAT3 translocation, which may be affected by the PI3K/Akt signaling pathway.

rHMGB1 has no effect on NMC apoptosis. Cardiac hypertrophy may lead to cardiomyocyte apoptosis during the heart failure process (35). In the present study, the apoptosis rate was measured using the TUNEL assay to detect TUNEL-positive nuclei and to determine whether rHMGB1 treatment induced NMC apoptosis. However, no significant differences in the number of TUNEL-positive nuclei were observed among the four groups (Fig. 5).

Discussion

The present study demonstrated that rHMGB1 induced NMC hypertrophy, decreased 14-3-3η protein levels and induced translocation of NFAT3 from the cytoplasm to the nucleus. The effects of rHMGB1 on NMC hypertrophy, 14-3-3η levels and NFAT3 translocation may be partially blocked by wortmannin, a specific PI3K inhibitor. However, rHMGB1 alone did not affect NMC apoptosis. Overall, the present results support the hypothesis that exogenous HMGB1 induces cardiomyocyte hypertrophy via the 14-3-3/PI3K/Akt/NFAT signaling pathway.

HMGB1 is a ubiquitous nuclear protein that is released from cell nuclei following tissue damage (36). Endogenous HMGB1 is located in the nucleus (37) and is actively secreted by innate immune cells (38) or other cells under stress conditions (6). Therefore, HMGB1 is found in cells and in the systemic
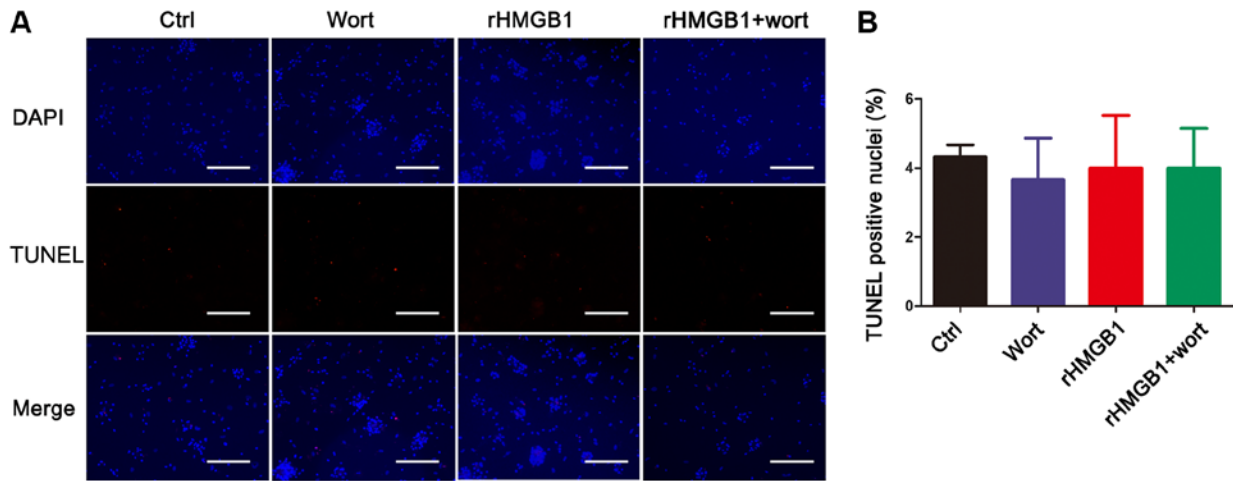
Figure 5. rHMGB1 has no effect on the apoptosis rate of neonatal mouse cardiomyocytes assessed using a TUNEL assay. (A) Fluorescence microscopic images of TUNEL-positive nuclei. Red indicates TUNEL-positive nuclei and blue indicates total nuclei (scale bar, 200 μm). The experiment was repeated (five independent experiments were performed). TUNEL-positive nuclei were counted in four fields for each experiment under a fluorescent microscope (n=12). (B) Data analysis of the number of TUNEL-positive nuclei from the different groups. One-way ANOVA was used to assess differences among the different groups. rHMGB1, recombinant high-mobility group box 1; TUNEL, terminal deoxynucleotidyl transferase dUTP nick-end-labeling; Wort, wortmannin; Ctrl, control; DAPI, 2-(4-amidinophenyl)-1H-indole-6-carboxamidine.

circulation. It has been reported that endogenous HMGB1 may serve an important role in myocardium pathology (39). In addition, patients with myocarditis display increased systemic HMGB1 levels, suggesting its involvement in the pathogenesis of inflammatory cardiomyopathy (2). However, the effects of secreted HMGB1 on the cardiovascular system remain unclear, and the effect of exogenous HMGB1 treatment on cardiomyocytes requires further investigation. The results of the present study revealed that rHMGB1 treatment increased ANP protein levels, BNP and ANP mRNA synthesis, and protein content per cell, highlighting its role in the induction of NMC hypertrophy. In the present study, HMGB1 increased the intracellular levels of ANP and BNP in cardiomyocytes. However, whether HMGB1 is able to enhance the secretion of ANP or BNP was not the main purpose of the present study; this should be analyzed *in vivo* in future studies. The aforementioned results suggest that both endogenous and exogenous HMGB1 serve a role in myocardial modifications, which is consistent with a previous study demonstrating that exogenous HMGB1 treatment induced cardiomyocyte survival in a murine myocardial infarction model (16).

In the present study, HMGB1 activated NFAT3 by promoting its translocation to the nucleus, thereby upregulating its nuclear expression. Additionally, it has been documented that NFAT3 is regulated by 14-3-3 proteins (25,26), exhibits inflammatory effects and induces pathological hypertrophy in cardiac myocytes (27-29).

14-3-3 proteins interact with several proteins, including PI3K, Akt and NFAT3 in diabetic cardiomyopathy (40). 14-3-3 proteins are dimeric phosphoserine-binding molecules separated into several isoforms, including the β, γ, ε, ζ, η, θ and σ isoforms (19). These proteins bind to their target proteins and modify their function by altering their intracellular localization and phosphorylation status (20). Several studies have concluded that 14-3-3 proteins, particularly the 14-3-3η isoform, are involved in diabetic cardiomyopathy (40,41). However, whether 14-3-3η is
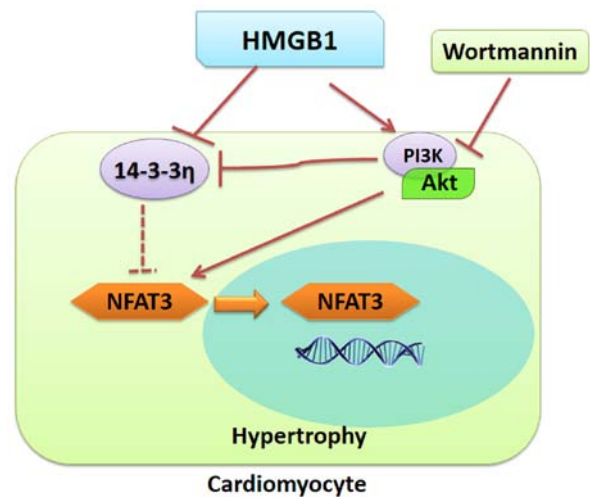

Figure 6. Proposed effects of rHMGB1 on cardiomyocyte hypertrophy. rHMGB1 may induce cardiomyocyte hypertrophy by regulating the 14-3-3/PI3K/Akt/NFAT3 signaling pathway. The red solid arrows and the solid T-shaped lines indicate the stimulatory and inhibitory effects, respectively. The dashed line indicates the probable effect. rHMGB1, recombinant high-mobility group box 1; NFAT3, nuclear factor of activated T cells 3.

involved in rHMGB1-induced hypertrophy, an independent predictor of cardiovascular morbidity and mortality, requires further investigation. The results of the present study revealed that the levels of total 14-3-3 proteins in NMCs did not change in the presence of rHMGB1. However, the protein levels of 14-3-3η were significantly decreased in rHMGB1-treated NMCs, resulting in significant induction of NMC hypertrophy. Therefore, the present results suggest that 14-3-3η, and not total 14-3-3, may serve a major role in rHMGB1-induced NMC hypertrophy.

NMCs were treated with a specific PI3K inhibitor prior to exposure to rHMGB1. Notably, the levels of 14-3-3η were partially preserved in rHMGB1-treated NMCs following wortmannin pretreatment. Additionally, wortmannin partially

inhibited NFAT3 nuclear translocation. The present results suggest that PI3K, Akt and NFAT3 may interact with 14-3-3η and may influence rHMGB1-induced hypertrophy. The proposed model of rHMGB1-mediated regulation of NMC hypertrophy is illustrated in Fig. 6.

Furthermore, it has been reported that cardiomyocyte hypertrophy may eventually lead to apoptosis (35). Therefore, a TUNEL assay was performed to determine the rHMGB1-induced apoptosis rate in NMCs. However, no statistically significant differences were observed in the NMC apoptosis rate between the Ctrl and the rHMGB1-treated groups. The present finding is consistent with a previous study demonstrating that HMGB1 does not induce cardiomyocyte apoptosis under normal conditions (42). However, it has been reported that endogenous HMGB1 contributes to ischemia-reperfusion-induced myocardial apoptosis (39). A potential explanation for these contrasting findings may reside in the different environments or distinct receptors on different cells. Therefore, further investigation is required to investigate the role of exogenous HMGB1 in different cell types.

In conclusion, the present study demonstrated that extracellular HMGB1 treatment induced NMC hypertrophy potentially through the 14-3-3η/PI3K/Akt/NFAT signaling pathway. Therefore, 14-3-3 may be an important factor that links HMGB1, PI3K/Akt and NFAT3 in cardiomyocytes.

Acknowledgements

Not applicable.

Availability of data and materials

The datasets used and/or during the present study are available from the corresponding author on reasonable request.

Authors' contributions

FS conceived the study. FS, MS and JZ performed the experiments. YL and JT analyzed the experimental data, assessed the raw data and confirm the authenticity of all the raw data. FS prepared the manuscript. All authors read and approved the final manuscript.

Ethics approval and consent to participate

The present experimental procedures were performed according to the ethical guidelines of the 1964 Declaration of Helsinki. All animal experiments were approved by the Animal Care and Welfare Ethics Committee of the Fourth Military Medical University (Xi'an, China).

Patient consent for publication

Not applicable.

Competing interests

The authors declare that they have no competing interests.

References

1. Biscetti F, Flex A, Alivernini S, Tolusso B, Gremese E and Ferraccioli G: The role of high-mobility group Box-1 and its crosstalk with microbiome in rheumatoid arthritis. Mediators Inflamm 2017: 5230374, 2017.
2. Bangert A, Andrassy M, Muller AM, Bockstahler M, Fischer A, Volz CH, Leib C, Göser S, Korkmaz-Icöz S, Zittrich S, et al: Critical role of RAGE and HMGB1 in inflammatory heart disease. Proc Natl Acad Sci USA 113: E155-E164, 2016.
3. Dong LY, Chen F, Xu M, Yao LP, Zhang YJ and Zhuang Y: Quercetin attenuates myocardial ischemia-reperfusion injury via downregulation of the HMGB1-TLR4-NF-kB signaling pathway. Am J Transl Res 10: 1273-1283, 2018.
4. Zhang W, Tao A, Lan T, Cepinskas G, Kao R, Martin CM and Rui T: Carbon monoxide releasing molecule-3 improves myocardial function in mice with sepsis by inhibiting NLRP3 inflammasome activation in cardiac fibroblasts. Basic Res Cardiol 112: 16, 2017.
5. Wu RN, Yu TY, Zhou JC, Li M, Gao HK, Zhao C, Dong RQ, Peng D, Hu ZW, Zhang XW and Wu YQ: Targeting HMGB1 ameliorates cardiac fibrosis through restoring TLR2-mediated autophagy suppression in myocardial fibroblasts. Int J Cardiol 267: 156-162, 2018.
6. Shen W, Zhou J, Wang C, Xu G, Wu Y and Hu Z: High mobility group box 1 induces calcification of aortic valve interstitial cells via toll-like receptor 4. Mol Med Rep 15: 2530-2536, 2017.
7. Lv Q, Li C, Mo Y and He L: The role of HMGB1 in heart transplantation. Immunol Lett 194: 1-3, 2018.
8. Su FF, Shi MQ, Guo WG, Liu XT, Wang HT, Lu ZF and Zheng QS: High-mobility group box 1 induces calcineurin-mediated cell hypertrophy in neonatal rat ventricular myocytes. Mediators Inflamm 2012: 805149, 2012.
9. Nehra S, Bhardwaj V, Kalra N, Ganju L, Bansal A, Saxena S and Saraswat D: Nanocurcumin protects cardiomyoblasts H9c2 from hypoxia-induced hypertrophy and apoptosis by improving oxidative balance. J Physiol Biochem 71: 239-251, 2015.
10. Fang X, Liu Y, Lu J, Hong H, Yuan J, Zhang Y, Wang P, Liu P and Ye J: Protocatechuic aldehyde protects against isoproterenol-induced cardiac hypertrophy via inhibition of the JAK2/STAT3 signaling pathway. Naunyn Schmiedebergs Arch Pharmacol 391: 1373-1385, 2018.
11. Wang S, Han HM, Pan ZW, Hang PZ, Sun LH, Jiang YN, Song HX, Du ZM and Liu Y: Choline inhibits angiotensin II-induced cardiac hypertrophy by intracellular calcium signal and p38 MAPK pathway. Naunyn Schmiedebergs Arch Pharmacol 385: 823-831, 2012.
12. Zwadlo C, Schmidtmann E, Szaroszyk M, Kattih B, Froese N, Hinz H, Schmitto JD, Widder J, Batkai S, Bähre H, et al: Antiandrogenic therapy with finasteride attenuates cardiac hypertrophy and left ventricular dysfunction. Circulation 131: 1071-1081, 2015.
13. Song L, Wang L, Li F, Yukht A, Qin M, Ruther H, Yang M, Chaux A, Shah PK and Sharifi BG: Bone marrow-derived tenascin-C attenuates cardiac hypertrophy by controlling inflammation. J Am Coll Cardiol 70: 1601-1615, 2017.
14. Gendy AM, Abdallah DM and El-Abhar HS: The potential curative effect of rebamipide in hepatic ischemia/reperfusion injury. Naunyn Schmiedebergs Arch Pharmacol 390: 691-700, 2017.
15. Raucci A, Di Maggio S, Scavello F, D'Ambrosio A, Bianchi ME and Capogrossi MC: The Janus face of HMGB1 in heart disease: A necessary update. Cell Mol Life Sci 76: 211-229, 2019.
16. Foglio E, Puddighinu G, Germani A, Russo MA and Limana F: HMGB1 inhibits apoptosis following MI and induces autophagy via mTORC1 inhibition. J Cell Physiol 232: 1135-1143, 2017.
17. Zhang L, Liu M, Jiang H, Yu Y, Yu P, Tong R, Wu J, Zhang S, Yao K, Zou Y and Ge J: Extracellular high-mobility group box 1 mediates pressure overload-induced cardiac hypertrophy and heart failure. J Cell Mol Med 20: 459-470, 2016.
18. Funayama A, Shishido T, Netsu S, Narumi T, Kadowaki S, Takahashi H, Miyamoto T, Watanabe T, Woo CH, Abe J, et al: Cardiac nuclear high mobility group box 1 prevents the development of cardiac hypertrophy and heart failure. Cardiovasc Res 99: 657-664, 2013.

19. Liao W, Wang S, Han C and Zhang Y: 14-3-3 proteins regulate glycogen synthase 3beta phosphorylation and inhibit cardiomyocyte hypertrophy. FEBS J 272: 1845-1854, 2005.
20. Jia H, Liang Z, Zhang X, Wang J, Xu W and Qian H: 14-3-3 proteins: An important regulator of autophagy in diseases. Am J Transl Res 9: 4738-4746, 2017.
21. Obsilova V, Kopecka M, Kosek D, Kacirova M, Kylarova S, Rezabkova L and Obsil T: Mechanisms of the 14-3-3 protein function: Regulation of protein function through conformational modulation. Physiol Res 63 (Suppl 1): S155-S164, 2014.
22. Sreedhar R, Arumugam S, Thandavarayan RA, Karuppagounder V, Koga Y, Nakamura T, Harima M and Watanabe K: Role of 14-3-3 η protein on cardiac fatty acid metabolism and macrophage polarization after high fat diet induced type 2 diabetes mellitus. Int J Biochem Cell Biol 88: 92-99, 2017.
23. Sreedhar R, Arumugam S, Thandavarayan RA, Giridharan VV, Karuppagounder V, Pitchaimani V, Afrin R, Miyashita S, Nomoto M, Harima M, *et al*: Myocardial 14-3-3 η protein protects against mitochondria mediated apoptosis. Cell Signal 27: 770-776, 2015.
24. Sreedhar R, Arumugam S, Thandavarayan RA, Giridharan VV, Karuppagounder V, Pitchaimani V, Afrin R, Harima M, Nakamura M, Suzuki K, *et al*: Depletion of cardiac 14-3-3 η protein adversely influences pathologic cardiac remodeling during myocardial infarction after coronary artery ligation in mice. Int J Cardiol 202: 146-153, 2016.
25. Chhabra S, Fischer P, Takeuchi K, Dubey A, Ziarek JJ, Boeszoermenyi A, Mathieu D, Bermel W, E Davey N, Wagner G and Arthanari H: (15)N detection harnesses the slow relaxation property of nitrogen: Delivering enhanced resolution for intrinsically disordered proteins. Proc Natl Acad Sci USA 115: E1710-E1719, 2018.
26. Faul C, Donnelly M, Merscher-Gomez S, Chang YH, Franz S, Delfgaauw J, Chang JM, Choi HY, Campbell KN, Kim K, *et al*: The actin cytoskeleton of kidney podocytes is a direct target of the antiproteinuric effect of cyclosporine A. Nat Med 14: 931-938, 2008.
27. Kumar S, Wang G, Liu W, Ding W, Dong M, Zheng N, Ye H and Liu J: Hypoxia-induced mitogenic factor promotes cardiac hypertrophy via calcium-dependent and hypoxia-inducible Factor-1α mechanisms. Hypertension 72: 331-342 2018.
28. Grund A, Szaroszyk M, Doppner JK, Mohammadi MM, Kattih B, Korf-Klingebiel M, Gigina A, Scherr M, Kensah G, Jara-Avaca M, *et al*: A gene therapeutic approach to inhibit CIB1 ameliorates maladaptive remodeling in pressure overload. Cardiovasc Res 115: 71-82, 2019.
29. Gelinas R, Mailleux F, Dontaine J, Bultot L, Demeulder B, Ginion A, Daskalopoulos EP, Esfahani H, Dubois-Deruy E, Lauzier B, *et al*: AMPK activation counteracts cardiac hypertrophy by reducing O-GlcNAcylation. Nat Commun 9: 374, 2018.
30. Su F, Shi M, Zhang J, Zheng Q, Zhang D, Zhang W, Wang H and Li X: Simvastatin protects heart from pressure overload injury by inhibiting excessive autophagy. Int J Med Sci 15: 1508-1516, 2018.
31. DeBosch B, Treskov I, Lupu TS, Weinheimer C, Kovacs A, Courtois M and Muslin AJ: Akt1 is required for physiological cardiac growth. Circulation 113: 2097-2104, 2006.
32. O'Neill BT, Kim J, Wende AR, Theobald HA, Tuinei J, Buchanan J, Guo A, Zaha VG, Davis DK, Schell JC, *et al*: A conserved role for phosphatidylinositol 3-kinase but not Akt signaling in mitochondrial adaptations that accompany physiological cardiac hypertrophy. Cell Metab 6: 294-306, 2007.
33. Gao RR, Wu XD, Jiang HM, Zhu YJ, Zhou YL, Zhang HF, Yao WM, Li YQ and Li XL: Traditional Chinese medicine Qiliqiangxin attenuates phenylephrine-induced cardiac hypertrophy via upregulating PPARγ and PGC-1α. Ann Transl Med 6: 153, 2018.
34. Schmittgen TD and Livak KJ: Analyzing real-time PCR data by the comparative C(T) method. Nat Protoc 3: 1101-1108, 2008.
35. Lu F, Xing J, Zhang X, Dong S, Zhao Y, Wang L, Li H, Yang F, Xu C and Zhang W: Exogenous hydrogen sulfide prevents cardiomyocyte apoptosis from cardiac hypertrophy induced by isoproterenol. Mol Cell Biochem 381: 41-50, 2013.
36. Hwang JH, Chu H, Ahn Y, Kim J and Kim DY: HMGB1 promotes hair growth via the modulation of prostaglandin metabolism. Sci Rep 9: 6660, 2019.
37. Muller S, Ronfani L and Bianchi ME: Regulated expression and subcellular localization of HMGB1, a chromatin protein with a cytokine function. J Intern Med 255: 332-343, 2004.
38. Tang D, Shi Y, Kang R, Li T, Xiao W, Wang H and Xiao XZ: Hydrogen peroxide stimulates macrophages and monocytes to actively release HMGB1. J Leukoc Biol 81: 741-747, 2007.
39. Xu H, Yao Y, Su Z, Yang Y, Kao R, Martin CM and Rui T: Endogenous HMGB1 contributes to ischemia-reperfusion-induced myocardial apoptosis by potentiating the effect of TNF-α/JNK. Am J Physiol Heart Circ Physiol 300: H913-H921, 2011.
40. Watanabe K, Thandavarayan RA, Gurusamy N, Zhang S, Muslin AJ, Suzuki K, Tachikawa H, Kodama M and Aizawa Y: Role of 14-3-3 protein and oxidative stress in diabetic cardiomyopathy. Acta Physiol Hung 96: 277-287, 2009.
41. Thandavarayan RA, Watanabe K, Ma M, Veeraveedu PT, Gurusamy N, Palaniyandi SS, Zhang S, Muslin AJ, Kodama M and Aizawa Y: 14-3-3 protein regulates Ask1 signaling and protects against diabetic cardiomyopathy. Biochem Pharmacol 75: 1797-1806, 2008.
42. Lin H, Shen L, Zhang X, Xie J, Hao H, Zhang Y, Chen Z, Yamamoto H, Liao W, Bin J, *et al*: HMGB1-RAGE axis makes no contribution to cardiac remodeling induced by pressure-overload. PLoS One 11: e158514, 2016.